# Development of methods for damage Identification in laminated composite structures

Tomás Miguel Pargana e Oliveira
tomasmiguelpo@tecnico.ulisboa.pt

Instituto Superior Técnico, Universidade de Lisboa, Portugal

November 2021

**Abstract**

Laminated composite materials are a staple of modern material development, with fibers stronger than most conventional materials being combined with resins to form versatile and efficient engineering structures. However, the advancements in material development must be accompanied by equally advanced methods for damage detection, as these materials develop inherently unique failure modes. This thesis aims to further the study of the use of modal shapes and their spatial derivatives to perform damage localization in laminated composite rectangular plates. Ansys® is used to perform Finite Element simulations of plates with several damage scenarios and damage mechanics models. Matlab® is used to post-process these simulations results, namely by calculating the derivatives using the Finite Difference Method, and applying three different Damage Indexes, including one that is being proposed here. To mimic experimental conditions and testing the resilience of the derivatives degrees, different noise levels are introduced in the results of the Finite Element simulations. A Quality Index is employed to quantitatively evaluate the solutions, mainly regarding the response to the introduced noise. The results show that the different Damage Detection Methods tested have comparable results in terms of quality with a higher degree of success when the analysis is made mode by mode, with a penalty in simplicity of analysis. These results also show that the damage detectability is higher when the damaged areas coincide with high displacement areas of the mode shapes and that higher noise levels have a more noticeable negative impact when employing higher order derivatives.

**Keywords:** Laminated composites, Modal analysis, Noise simulation, Finite elements, Damage localization, Finite Differences

## 1. Introduction

Composite materials are, by definition, the result of the combination of more than one type of material. Laminated composites combine high strength fibers, such as carbon or glass, with a resin matrix, which binds the fibers in place and evenly distributes the loads in each direction. As the fibers are often laid out in the same direction in thin plies, each ply has an anisotropic nature, with the fibers' direction being much more rigid than the others; for this reason, several plies are stacked in multiple orientations to make a laminated part which can respond to different load cases and perform as intended [1]. The resultant materials have been having a considerable impact on the development of engineering solutions in the past decades, in all areas of activity, most notably in the aerospace industry, with examples such as the Boeing 787 aircraft, which is composed by 50% composite materials[2]. The main advantages of laminated composites include superior specific strength and stiffness [3], with the main drawback being the high production costs.

The nature of laminated composites originates unique damage mechanics, the most notable of which are fiber-matrix debonding and delamination, as studied and modelled by previous authors [4]. The damage detection and location methods proposed here are based on vibration modes, which produce specific mode shapes and natural frequencies, which is an approach that has been used for a few decades for different types of materials[5]. The damage detection is based on the difference between the mode shapes of intact and damaged plates, as well as their corresponding spatial derivatives calculated through the finite difference method. The use of these techniques has been continuously studied for several years for the use on beams, mainly of aluminum, with both numerical and experimental validation of the results, most notably by authors such as Pandey et al. [6], Abdel Wahab and De Roeck [7], Sazonov and Klinkhachorn [8]. More recently, other authors such as Araújo dos Santos et al. [9], Moreno-García et al. [10] applied them to

composite plates, which is the object of study of this work, again with both numerical and experimental data for a deeper understanding of the usefulness of these techniques.

The damage detection methods are performed on Finite Elements simulations run in Ansys® and post-processed using Matlab®, for carbon fibre-epoxy rectangular plates with specific material and geometric properties. The damage is simulated on specific areas on one or all plies of the laminate, by manipulating the elastic constants through one of two damage mechanics approaches. In order to have a more comprehensive understanding of the capabilities of the chosen methods, different variables are tested, such as boundary conditions, damage severity and location, damage mechanics model, damage depth, and introduction of noise in the measurements to test the methods for field applications. Each variable that is written with a tilde (e.g. $\tilde{w}$) corresponds to a damaged plate.

## 2. Damage Detection Methods

### 2.1. Laminated composite materials, natural frequencies and mode shapes

Composite laminated parts are designed to perform a specific task, and must meet certain structural, electrical or thermal requirements, amongst others. The fiber's and resin's properties, as well as their respective volumetric concentrations on the plies contribute to the material properties of the composite; there are different theories on the exact weights of these contributions, however they are not explored here, as the material properties used are those of already studied and characterized composite plies. The plate simulated in this analysis had its layer sequence and orientation proposed by Ladevèze and Lubineau [4] to study one of the damage mechanics models used here, being the plate dimensions, mesh size, damage size and ply properties as the ones used by Moreno-García et al. [10] to apply the same type of modal analysis. The plate has a length and width of 400 mm by 200 mm, a thickness of 0.75 mm and a stacking of $[90/0_2]_s$. The plies are composed of an AS4/Epoxy, with $E_1 = 138$ GPa, $E_2 = 10.3$ GPa, $G_{12} = 6.9$ GPa, $\nu_{12} = 0.30$ and $\rho = 1.55$ g/cm3. For the vibration analysis, the four edges of the plate are clamped, except for some aspects on which the behaviour of a free plate is also analyzed.

The proposed damage detection methods are based on the dynamic behaviour of plates, which, when excited to their natural frequencies, resonate and produce their respective mode shapes. The difference between the behaviour of undamaged and damaged plates should be detectable by comparing the frequencies and mode shapes of both, as well as the spatial derivatives of the mode shapes. As a general notion, it can be assumed that a less rigid structure will have lower natural frequencies to a similar but more rigid one, and as such the prediction is that the natural frequencies are lower for the damaged plates.

### 2.2. Finite Element Method

The numerical simulation of the laminated plate is made using the commercial software Ansys®, though a Mechanical APDL® script. The plate's domain is divided in SHELL181 square elements with a side dimension of 5 mm, being the lay-up (called Section in the software) defined according to the staking sequence and the layer properties specifications - for both undamaged and damaged laminates. The element size of 5 mm is chosen according to the study of the optimal sampling presented by Moreno-García et al. [10] with important compromises made due to the fact that several different degrees of derivation are used and the computation time needs to be managed - with the chosen sizing, each simulation and computation routine takes from 5 minutes to 2 hours, depending on the chosen index. This choice intends to minimize the influence of the noise and errors in the data. It should be noted that experimental techniques usually only allow the measuring of the mode shapes and modal rotations [11]; this justifies the need to apply numerical differentiation techniques to experimental data to obtain the modal curvature and higher degree derivatives.

The damage is simulated by multiplying the elastic constants of each ply by coefficients called damage parameters, being each damage parameter selected according to the employed model of damage mechanics. The first method used here is proposed by Ladevèze and Lubineau [4] and it studies the microcracking in the matrix while the comparatively much stronger fibers are considered intact; several sets of values are tested for this model, and the one selected for further analysis is denominated DC1, on which $\tilde{E}_2 = E_2 * 0.21$, $\tilde{G}_{12} = G_{12} * 0.42$, and the remaining elastic constants are kept unchanged. The method used by Moreno-García et al. [10] uses a much simpler approach of multiplying all of the elastic constants, except the Poisson's ratio, by a damage parameter, such that $\left\|[\tilde{D}_{(e)}]\right\| = (1 - d^{(e)}) * \left\|[D_{(e)}]\right\|$; as before, different values of $d^{(e)}$ are tested and the one which is found most suitable is denominated DC2 where $d^{(e)} = 0.7$; through the analysis of the damage indices, it has been concluded that DC2 is about ten times more severe than DC1, which is a difference suitable to test the response of the damage detection methods to different severity levels.

### 2.3. Finite difference method

The employed damage indices are based on the differentiation of the transverse displacement of each

node on the plate. The numerical differentiation process chosen for this operation is the Finite Difference method, which uses the values of the displacement and their spacing, uniform in each direction, to approximate the derivatives.

The formula for the first derivative can be found on Equation (1), and the subsequent degrees are calculated by substituting the variable on the equation by the equation itself (i.e. $f''(x) = f'(f'(x))$) and simplifying the resulting fraction. To obtain different values of accuracy in the operation, different orders of the finite differences can be used. However they require more points, thus disabling the possibility to compute the derivative on nodes close to the edges of the plate. In view of this, a choice was made to restrict the computations using only the second order central finite difference.

$$\frac{\partial w}{\partial x} = \frac{-\frac{1}{2}w(x-h,y) + \frac{1}{2}w(x+h,y)}{h} \tag{1}$$

2.4. Damage indices

Three different damage indices are used, two of which were already applied in previous studies and one is proposed in this work.

Moreno-García et al. [10] proposed the use of the DFD (Difference in Field Derivatives) damage index, which calculates the derivatives in the $x$ direction up to the fourth order, as shown in Equation (2), for each mode.

$$DFD_q^{(P)}(x,y) = \left| \frac{\partial^P w_q(x,y)}{\partial x^P} - \frac{\partial^P \tilde{w}_q(x,y)}{\partial x^P} \right| \tag{2}$$

Araújo dos Santos et al. [9] proposed the use of three damage indices which calculate the difference between the averages through the first ten modes of the displacements and first two derivatives, as shown in Equation (3), where in each derivative order the Euclidean norm of the derivative's vector's components is used, and the derivative vectors are shown in Equation (4); here, the equivalent vectors for the damaged plates are implied and are calculated in the exact same way.

$$TD(x,y) = \frac{1}{n}\sum_{q=1}^{n} |w_q(x,y) - \tilde{w}_q(x,y)| \tag{3a}$$

$$SD(x,y) = \frac{1}{n}\sum_{q=1}^{n} \left| \|\boldsymbol{\theta}_q(x,y)\|_2 - \left\|\tilde{\boldsymbol{\theta}}_q(x,y)\right\|_2 \right| \tag{3b}$$

$$CD(x,y) = \frac{1}{n}\sum_{q=1}^{n} \left| \|\boldsymbol{\kappa}_q(x,y)\|_2 - \|\tilde{\boldsymbol{\kappa}}_q(x,y)\|_2 \right| \tag{3c}$$

$$\boldsymbol{\theta}_q(x,y) = \begin{Bmatrix} (\theta_x)_q(x,y) \\ (\theta_y)_q(x,y) \end{Bmatrix} = \begin{Bmatrix} \dfrac{\partial w_q(x,y)}{\partial x} \\ \dfrac{\partial w_q(x,y)}{\partial y} \end{Bmatrix} \tag{4a}$$

$$\boldsymbol{\kappa}_q(x,y) = \begin{Bmatrix} \dfrac{-\partial^2 w_q(x,y)}{\partial x^2} \\ \dfrac{-\partial^2 w_q(x,y)}{\partial y^2} \\ -2\dfrac{\partial^2 w_q(x,y)}{\partial x \partial y} \end{Bmatrix} \tag{4b}$$

The SFD (Sum of Field Derivatives) method consists of a mix of the characteristics of both the previous ones: the performing of the derivatives in one direction only up to the fourth order, and the use of the average displacements of the first ten modes, as shown in Equation (5).

$$SFD^{(P)}(x,y) = \left| \frac{1}{n}\sum_{q=1}^{n}\left(\frac{\partial^P w_q(x,y)}{\partial x^P}\right) - \frac{1}{n}\sum_{q=1}^{n}\left(\frac{\partial^P \tilde{w}_q(x,y)}{\partial x^P}\right) \right| \tag{5}$$

2.5. Results post-processing

The FE simulation results are post-processed in Matlab® to calculate the derivatives and the damage indices, as well as creating figures that show the results.

### 2.5.1 Results quality index

For a single damaged area, a quality index $\mu$ was proposed by Moreno-García et al. [12], which measures how concentrated the peaks of the damage index are, and is calculated as shown in Equation (6). $DI$ is used to represent the nodal value of any damage index is chosen to apply this method, which is normalized to 1, as denoted by the hat, and NN is the number of nodes.

$$\mu = 1 - \frac{\sum_{k=1}^{NN} \hat{DI}}{NN}\ ,\ \hat{DI} \leq 1 \tag{6}$$

Paired with this quality index, a damage severity indicator is used, which is the maximum value of the damage index found in a specific damage case. This indicator is a better tool to compare damage cases, which sometimes show similar quality in detection. Both are used in context, using the figures to have a qualitative evaluation of the quality, as well as in comparison with different damage cases.

### 2.5.2 Noise simulation

The present simulations, as well as the set up lab conditions, have very little to no noise or interference. These conditions are invaluable to test the damage indices performance, however they do not account for the parallel between the sensitivity to small disturbances to the mode shapes, of which both damage and noise are comprised. To test the resilience of the chosen methods to the presence of noise, a randomized field of values is added to the displacement field, with a mean of 0 and a standard deviation of $10^{-6}$. As the displacements are normalized to 1, this level of noise doesn't have a noticeable impact on the results of any of the operations performed; thus, the defined value of noise is multiplied by a noise level $NL$, taking values from 1 to 10000.

### 2.5.3 Damage depth variation

The damage scenarios in the simulations described so far in the literature are comprised of a manipulation of the elastic constants on all plies on the laminate, on a specific area. However, for field applications, a study on the behaviour of the damage indices when the damage in contained in the inside layers is relevant, as this would hamper visual detection of the damage. For this reason, simulations are run where the damage is present in only one of the six layers of the laminate, and the damage detectability is compared.

## 3. Results

The mode shapes 1 and 7, as well as the average of the first ten modes, are shown in Figure 1; these two modes show very different behaviours of the displacement field across the plate, and should thus provide different responses from the damage index DFD.

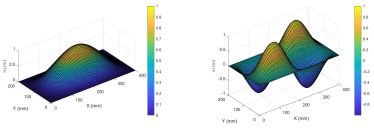

(a) Mode 1 (b) Mode 7 (c) Average of the first ten modes.

Figure 1: Displacement fields.

3.1. Damage indices

### 3.1.1 DFD index

As this index is used to perform the damage detection on a mode-by-mode basis, only the most significant cases are shown here. Figures 2 and 3 show the response of the DFD damage index to a center damage scenario, with DC1. As the behaviour of the two mode shapes on the center of the plate is so different, so is the damage detection: Mode 1 gives a much clearer detection than Mode 7, and shows effective damage detection using rotations ($DFD_q^{(1)}$), whereas using Mode 7 the detection only becomes effective using the curvatures ($DFD_q^{(2)}$) or the third derivative of the displacements ($DFD_q^{(3)}$).

Figure 4 shows the damage detection of a center + corner damage scenario, where both damaged areas are equal in size and damage severity, using the curvatures. Modes 1 and 8 show a very distinct response to the damage, as the former highlights only the center damaged area, and the latter shows similar peaks for both. For each one of the first ten modes, more diverse responses to this situation can be found, illustrating the importance of having several modes to ensure that no areas are prone to concealing damage.

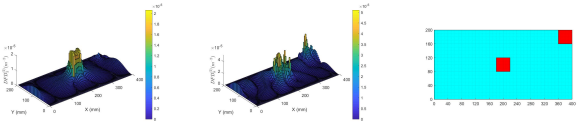

(a) $DFD_1^{(2)}$ (b) $DFD_8^{(2)}$ (c) Damage Scenario.

Figure 4: Center + Corner damage scenario, DC1.

### 3.1.2 TD, SD and CD indices

As these damage indices require the average of the first ten modes to be calculated, no specific modes need to be selected. Figures 5 and 6 show the response of these damage indices to a center damage scenario with DC1 and DC2, respectively. The use of the displacements (TD) provides no meaningful and clear damage localization. However, the rotations (SD) and curvatures (CD) show increasing clarity on the peaks on the damaged area, being this more visible for the curvature, justified by its higher order derivative.

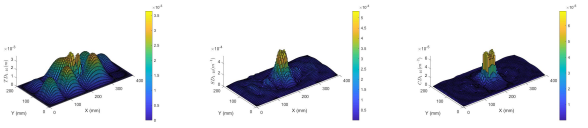

(a) $TD_{1-10}$ (b) $SD_{1-10}$ (c) $CD_{1-10}$

Figure 5: Center damage scenario, DC1.

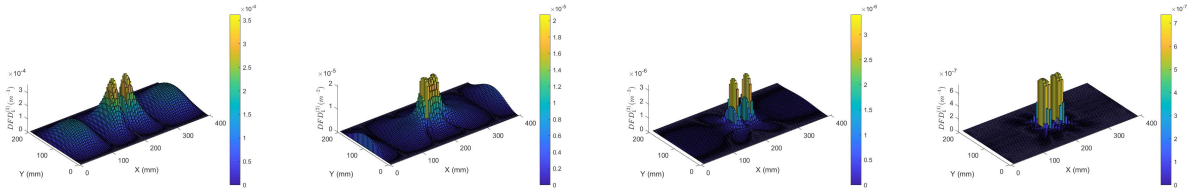

(a) $DFD_1^{(1)}$ (b) $DFD_1^{(2)}$ (c) $DFD_1^{(3)}$ (d) $DFD_1^{(4)}$

Figure 2: Center damage scenario, DC1, Mode 1.

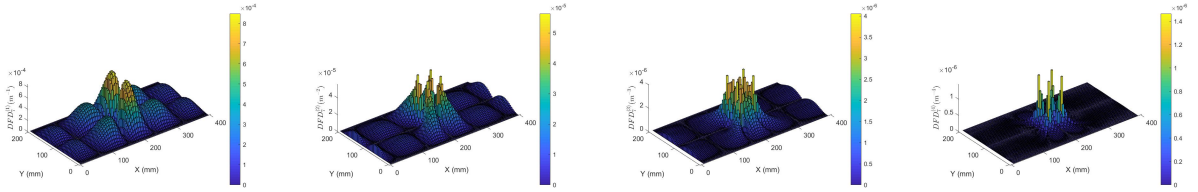

(a) $DFD_7^{(1)}$ (b) $DFD_7^{(2)}$ (c) $DFD_7^{(3)}$ (d) $DFD_7^{(4)}$

Figure 3: Center damage scenario, DC1, Mode 7.

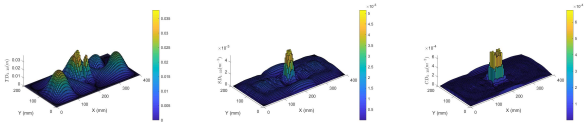

(a) $TD_{1-10}$ (b) $SD_{1-10}$ (c) $CD_{1-10}$

Figure 6: Center damage scenario, DC2.

Figure 7 shows the response of these indices to a center + corner damage scenario, with the two damaged areas being the same size and severity. The center damage is much more pronounced in this detection, which is likely a result of the higher sensitivity of most of the mode shapes to this area. These indices show this clear disadvantage, where only one figure can be analyzed, and the blind spots created by the majority of the mode shapes can not be avoided; however, this presents a much higher simplicity in analysis, which can increase efficiency in damage detection if the blind spots are known and accounted for.

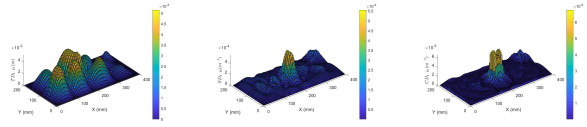

(a) $TD_{1-10}$ (b) $SD_{1-10}$ (c) $CD_{1-10}$

Figure 7: Center + corner damage scenario, DC1.

### 3.1.3 SFD index

The response of this damage index to a center damage scenario with DC1 can be seen on Figure 8; as these figures show a very clear damage localization for this damage case and all degrees of derivative, the same happens when DC2 is applied, only with higher values on the peaks.

The results with SFD damage index, depicted in Figures 8 and 9, show a clear identification of damage in the center scenario and both locations of damage in center + corner damage scenario, being the damage detection more clear with the derivative order increase. If we compare the results of the SFD damage index with the ones obtained with the other damage indices for the second damage scenario, the peaks at center of the plate are less noticeable than the ones at the corner. In this case, it is possible to identify both damages starting from the second order derivative, contrary to the other damage indices.

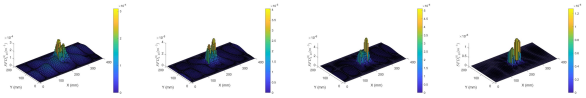

(a) $SFD_{1-10}^{(1)}$ (b) $SFD_{1-10}^{(2)}$ (c) $SFD_{1-10}^{(3)}$ (d) $SFD_{1-10}^{(4)}$

Figure 8: Center damage scenario, DC1.

Just as when using the TD, SD and CD indices, the tendency of the majority of the modes is to be more sensitive to the center damage than that on the corner, which creates a blind spot. In this case, the higher number of degrees of derivation is shown to have a positive impact on the detectability of both damaged areas.

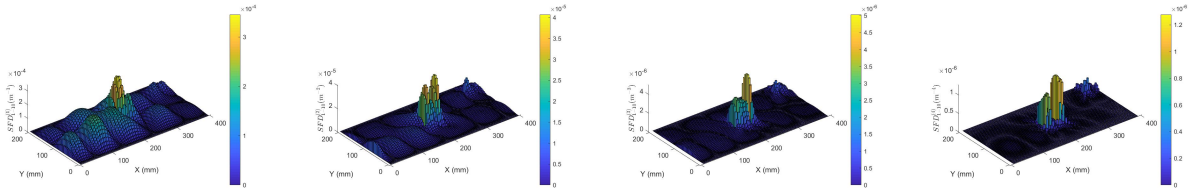

(a) $SFD^{(1)}_{1-10}$ (b) $SFD^{(2)}_{1-10}$ (c) $SFD^{(3)}_{1-10}$ (d) $SFD^{(4)}_{1-10}$

Figure 9: Center + corner damage scenario, DC1.

### 3.2. Frequency analysis

All simulations run produced lower frequencies for the damaged plates than those of the undamaged plates, and the same happens between DC1 and DC2, for all modes, as listed on Table 1. Figure 10 shows the average displacement on all nodes of the damaged area (for an undamaged plate) for each mode with columns, and the value of the relative frequency difference with lines, for both the clamped plate that has been studied so far and one that is free; this shows a correlation between the displacement and the difference in frequency, although stronger for the more severe damage case DC2 and weaker for the free plate, which suggests that the different values of FD for the modes can be used along with the mode shapes to locate damage, if the only measurements available are those of the frequencies.

Table 1: Natural frequency comparison for DC1 and DC2

| Mode | $f_q$(Hz) | ${}^1\tilde{f}_q$(Hz) | ${}^1\text{FD}_q$ | ${}^2\tilde{f}_q$(Hz) | ${}^2\text{FD}_q$ |
|---|---|---|---|---|---|
| 1 | 159,87 | 159,64 | 0,14% | 153,92 | 3,72% |
| 2 | 178,93 | 178,87 | 0,03% | 178,57 | 0,20% |
| 3 | 224,44 | 223,59 | 0,38% | 216,93 | 3,35% |
| 4 | 301,59 | 301,29 | 0,10% | 298,74 | 0,94% |
| 5 | 409,54 | 407,69 | 0,45% | 396,34 | 3,22% |
| 6 | 433,61 | 433,49 | 0,03% | 426,92 | 1,54% |
| 7 | 446,03 | 445,48 | 0,12% | 445,12 | 0,20% |
| 8 | 473,75 | 473,48 | 0,06% | 469,11 | 0,98% |
| 9 | 524,20 | 522,78 | 0,27% | 521,64 | 0,49% |
| 10 | 546,23 | 545,20 | 0,19% | 535,35 | 1,99% |

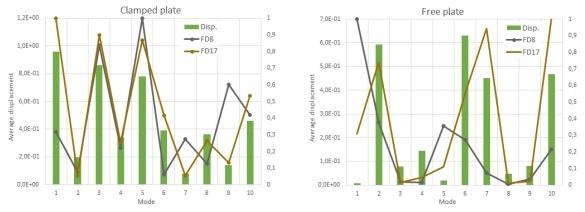


(a) Clamped plate (b) Free plate

Figure 10: Average displacement on the damaged area.

### 3.3. Influence of noise on detection

This analysis is made in two complementary approaches: a qualitative analysis of the figures depicting the damage indices and a statistical analysis of the behaviour of the quality index $\mu$, according to different noise levels. Figure 11 shows the borderline between detectable and undetectable damage, which is found to be at $\mu = 0.85$ across all differentiation orders and for multiple damage cases.

In order to obtain statistically relevant data regarding the behaviour of the derivative degrees when dealing with each noise level, 200 different simulations are performed for each noise level, where in each one a novel random field of noise is added to the mode shapes and the damage indices are calculated. This minimizes the impact that incidental high or low values of noise could have on the results. Figure 12 shows the average of the quality index $\mu$ for the 200 simulations, and there is a clear correlation between derivative order and resilience to noise in the measurements, where the first derivative has a lower quality damage detection, but is also much more immune to noise - more that 10x higher than the fourth derivative of the displacements. While using the higher order derivatives produces clearer damage detection, their sensitivity to the disturbances in the mode shapes caused by the presence of damage is also a weakness when dealing with the disturbance of noise; this dichotomy underlines the importance of having reliable and precise measurements to produce good quality damage detection.

### 3.4. Influence of damage depth

Using the SFD damage index, the maximum value of the index was found for six simulations, each of which corresponds to each one of the plies of the laminate being damaged, for a center damage scenario with DC1. The results shown in Figure 13 reveal a clear decrease in detectability when the damage is located in the center plies for all derivative orders, by a factor of 10 to 100, being the 1 and 6 the top and bottom layers, respectively. Having in mind the motivation of this analysis - the perceived lower visibility of damage in the interior plies -, these results suggest that modal analysis, in the form that

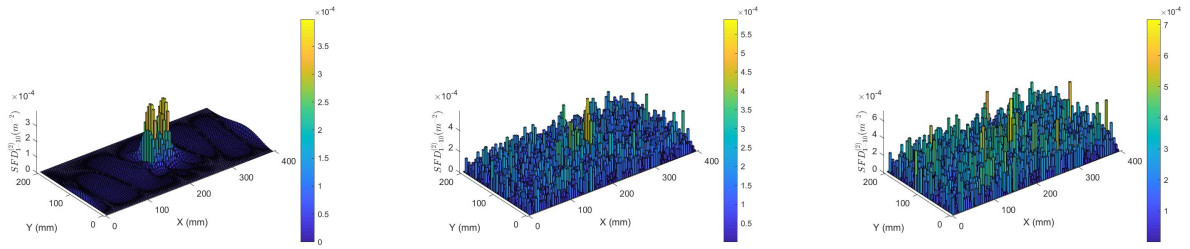


(a) NL=0, $\mu = 0.963$ (b) NL=3000, $\mu = 0.875$ (c) NL=5000, $\mu = 0.8348$

Figure 11: Damage detection with noise, $SFD^{(2)}_{1-10}$, DC2.

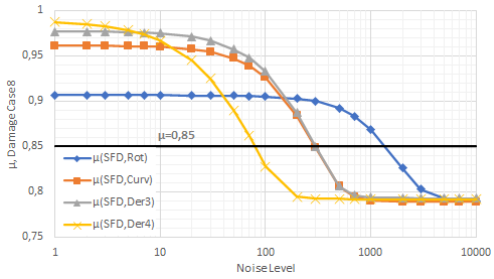


Figure 12: Detection quality according to noise level.

is proposed here, may not be the most suitable solution to detect this type of damage. Moreover, if one wants to detect damage in interior layers of a laminate, the quality of measurements are of utmost importance, since noisy data will easily mask the perturbations due to damage.

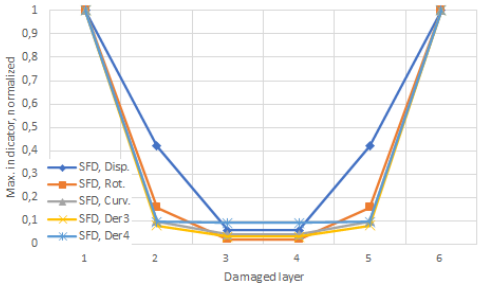


Figure 13: Damage severity according to damage depth.

## 4. Conclusions

Several aspects of the use of modal analysis for damage detection on composite plates are explored in this work, namely the use of different derivative techniques, the importance of pairing a quantitative analysis of the values of interest with the qualitative analysis of the generated figures, the importance of studying the mode shapes for a more comprehensive evaluation of the results - both for the damage indices and the frequency -, and some limitations of these techniques, namely the influence of noise and damage depth of the quality of the detection. A new damage index is proposed, which shows improved quality of multiple damage detection. A study on the influence of damage depth on detection was also successfully performed, examples of which have not been found in the reviewed literature.

Future work in this area should take into account some aspects which are not discussed here, such as measurement techniques for field applications, noise or error quantification for the modal shapes and frequency values, the testing of more complex structures to test the derivation process in different conditions, and validating the data processing on real-world setups.


## Acknowledgements

The author would like to thank the thesis advisor, Prof. Dr. José Viriato dos Santos for his guidance and insights.

The author's family and friends have also had an important role in the success of this thesis, of growth and motivation, and without them this project would have hardly come to fruition.


## References


[1] Alan Baker, Stuart Dutton, and Donald Kelly. *Composite Materials for Aircraft Structures*. American Institute of Aeronautics and Astronautics, Inc., $2^{nd}$ edition, 2004. ISBN:1-56347-540-5.

[2] Justin Hale. Boeing 787 from the ground up, 2008. URL `https://www.boeing.com/commercial/aeromagazine/articles/qtr_4_06/article_04_2.html`. [Online; accessed 26-October-2021].

[3] A. Brent Strong. *Fundamentals of Composites Manufacturing - Materials, Methods, and Applications*. Society of Manufacturing Engineers (SME), 2nd edition edition, 2008. ISBN 9781613449882.

[4] Pierre Ladevèze and Gilles Lubineau. On a damage mesomodel for laminates: micromechanics basis and improvement. *Mechanics of Materials*, 35(8):763–775, 2003. ISSN 0167-6636. doi: 10.1016/S0167-6636(02)00204-1. Multi-scale Modeling of Materials.

[5] Y. Zou, L. Tong, and G.P. Steven. Vibration-based model-dependent damage (delamination) identification and health monitoring for composites structures. *Journal of Sound and Vibration*, 230(2):357–378, 2000. ISSN 0022-460X. doi: https://doi.org/10.1006/jsvi.1999.2624.

[6] A.K. Pandey, M. Biswas, and M.M. Samman. Damage detection from changes in curvature mode shapes. *Journal of Sound and Vibration*, 145(2):321–332, 1991. ISSN 0022-460X. doi: https://doi.org/10.1016/0022-460X(91)90595-B.

[7] M.M. Abdel Wahab and G. De Roeck. Damage detection in bridges using modal curvatures: Application to a real damage scenario. *Journal of Sound and Vibration*, 226(2):217–235, 1999. ISSN 0022-460X. doi: https://doi.org/10.1006/jsvi.1999.2295.

[8] Edward Sazonov and Powsiri Klinkhachorn. Optimal spatial sampling interval for damage detection by curvature or strain energy mode shapes. *Journal of Sound and Vibration*, 285 (4):783–801, 2005. ISSN 0022-460X. doi: https://doi.org/10.1016/j.jsv.2004.08.021.

[9] J.V. Araújo dos Santos, H.M.R. Lopes, M. Vaz, C.M. Mota Soares, C.A. Mota Soares, and M.J.M. de Freitas. Damage localization in laminated composite plates using mode shapes measured by pulsed tv holography. *Composite Structures*, 76(3):272 – 281, 2006. ISSN 0263-8223. doi: https://doi.org/10.1016/j.compstruct.2006.06.034.

[10] P. Moreno-García, J.V. Araújo dos Santos, and H. Lopes. A new technique to optimize the use of mode shape derivatives to localize damage in laminated composite plates. *Composite Structures*, 108:548 – 554, 2014. ISSN 0263-8223. doi: https://doi.org/10.1016/j.compstruct.2013.09.050.

[11] H. Lopes, J.E. Ribeiro, and J. Santos. Interferometric techniques in structural damage identification. *Shock and Vibration*, 19:835–844, 2012. doi: 10.3233/SAV-2012-0692.

[12] P. Moreno-García, H. Lopes, and J.V. Araújo dos Santos. Application of higher order finite differences to damage localization in laminated composite plates. *Composite Structures*, 156: 385 – 392, 2016. ISSN 0263-8223. doi: https://doi.org/10.1016/j.compstruct.2015.08.011.